

Automated Phytosensing: Ozone Exposure Classification Based on Plant Electrical Signals

Till Aust,¹ Eduard Buss,¹ Felix Mohr,² and Heiko Hamann¹

Abstract—In our project *WatchPlant*, we propose to use a decentralized network of living plants as air-quality sensors by measuring their electrophysiology to infer the environmental state, also called phytosensing. We conducted in-lab experiments exposing ivy (*Hedera helix*) plants to ozone, an important pollutant to monitor, and measured their electrophysiological response. However, there is no well established automated way of detecting ozone exposure in plants. We propose a generic automatic toolchain to select a high-performance subset of features and highly accurate models for plant electrophysiology. Our approach derives plant- and stimulus-generic features from the electrophysiological signal using the *tsfresh* library. Based on these features, we automatically select and optimize machine learning models using *AutoML*. We use forward feature selection to increase model performance. We show that our approach successfully classifies plant ozone exposure with accuracies of up to 94.6% on unseen data. We also show that our approach can be used for other plant species and stimuli. Our toolchain automates the development of monitoring algorithms for plants as pollutant monitors. Our results help implement significant advancements for phytosensing devices contributing to the development of cost-effective, high-density urban air monitoring systems in the future.

I. INTRODUCTION

Since decades city populations are increasing at a fast pace, a phenomenon called urbanization.¹ One effect is increased traffic volume, which negatively impacts air quality. For example, in Europe just under two thirds of air pollution is accounted to traffic² and up to a third of European citizens are exposed to concentrations of air pollutants that exceed the European Union’s air quality standards, especially due to particulate matter and ozone.³ Hence, in addition to ongoing efforts to reduce pollution, also suitable air pollution monitoring techniques are needed to identify potential hazards early and to enable swift action [1]. Usually, such techniques incorporate expensive, fixed monitoring stations that provide highly accurate measurements with the drawback of low spatial resolution [2]. Hence, there is a paradigm shift towards more decentralized measurement approaches but a fundamental challenge remains in finding cost-effective methods to monitor all pollutants accurately [3]. Another approach addressing low spatial resolutions is to use mobile pollution

sensing systems. However, the increased spatial resolution comes with a tradeoff of reduced temporal resolution.

In our EU-funded project *WatchPlant* [4], [5] (2021-2024) we address both the challenge of measuring many pollutants in an inexpensive and effective way and the tradeoff of temporal and spatial resolution by proposing a network of low-cost bio-hybrid air-quality sensor nodes. Our vision is to deploy these air-quality sensor nodes densely throughout the city (possible due to their low-cost) and connecting all of them to aggregate pollution information for real-time monitoring to help policy makers to decide and inform citizens about potential hazards, for example, via their smart phones. By engaging citizens and avoiding private data collection (e.g., connection history) we mitigate ethical concerns. We anticipate a positive ecological impact as our biohybrid system promotes the expansion of urban green spaces. One biohybrid air-quality sensor node consists of an electronic device, our *PhytoNode* [6], [7], and a natural plant (in our case *Hedera helix*). The *PhytoNode* is a light-weight and inexpensive sensor used for phytosensing. In phytosensing the electric physiology of living plants is measured to sense, for example, the environmental conditions [8]. One advantage of phytosensing is that we can potentially infer multiple pollutants, which usually requires multiple different sensing devices, by only measuring one natural plant. A cost-effective and robust phytosensing approach is to measure electric differential potentials holistically across the entire plant. This can be done, for example, by inserting two needles as electrodes, one close to a leaf and one close to the bottom of the plant’s stem. A remaining challenge is to infer the environmental stimulus based on the measured holistic electric differential potential because this macroscopic level of electric physiology in plants is neither well studied nor thoroughly understood as of now [9].

Due to the recent successes of machine learning (ML) across many domains [10], [11], also several studies applied ML to analyze holistic plant electrophysiology. Most studies utilize phytosensing in the context of agriculture, for example, to detect drought stress using support vector machines [12], ensemble boosted tree classifiers [13], or (extreme) gradient boosting [14], [15]. Other studies utilize deep neural networks to detect salt stress [16], [17], nitrogen deficit [18], soil moisture [19] or other abiotic stressors [20] (classical machine learning approaches for abiotic stressors [21], [22]).

Fewer studies consider phytosensing in the context of air pollution monitoring, by experimenting with gas stimuli [23]. *Chatterjee* et al. [24] experimented with tomato plants and exposed them, among other stimuli, to ozone (16 ppm, that is, 266 times the threshold for preserving the citizen health

¹Till Aust, Eduard Buss and Heiko Hamann are with the Department of Computer and Information Science, University of Konstanz, Konstanz, Germany. {till.aust, eduard.buss, heiko.hamann}@uni-konstanz.de

²Felix Mohr is with the Faculty of Engineering, Universidad de La Sabana, Chia, Colombia. felix.mohr@unisabana.edu.co

¹<https://unhabitat.org/wcr/>

²<https://www.eea.europa.eu/highlights/emissions-from-road-traffic-and>

³<https://www.eea.europa.eu/soer/2015/europe/urban-systems>

stated by the EU⁴) for one minute every 2 hours. *Chatterjee et al.* propose to use discriminant analysis classifiers to classify ozone pollution based on 11 features, with background subtraction, derived from the plant electrical signal. Depending on the selected features and classifiers, they can distinguish between ozone and other stimuli (different concentrations of sodium chloride and sulfuric acid) with an accuracy of up to 95 %. This work has been extended by using more statistical features [25], curve fitting coefficients as features [26], or different classifiers [27]. However, they did not study whether a stimulus can be distinguished from the resting state (i.e., no stimulus).

Dolfi et al. [28] propose a two step detection algorithm to assess ozone air pollution based on plant electrical signals. In a first step, they use a derivative-based algorithm for change detection in the signal. If a change is detected, they employ correlation waveform analysis to assess if the change is due to ozone pollution. They exposed *Ligustrum texanum* and *Buxus macrophylla* to either ozone concentrations of 200 ppb or gradually increasing ozone levels from 50 to 200 ppb. They achieve an overall detection accuracy of 87 %. However, their method requires to manually select three plant specific thresholds for the detection algorithm and plant specific waveform responses for the correlation measure. They also did not study if this methods generalizes to other pollutants or stimuli.

All the above studies have in common that they choose the ML models ad hoc without providing a rationale for choosing one over another. They appear to have selected a functioning model through manual parameter adjustments or by comparing a restricted set of seemingly randomly chosen models. As a possible solution we propose to use automated machine learning (AutoML). Methods of AutoML automatically compose and parameterize ML algorithms to optimize a provided metric [29]. There are implemented frameworks, such as, auto-sklearn [30], [31] and GAMA [32]. More recently *Mohr and Wever* [33] proposed the Naive AutoML framework which yields similar performance while significantly reducing computation time.

We aim to close the gap of automatically finding a model that can classify external stimuli based on (holistic) plant electric differential potentials to contribute to decipher the plant physiology. We propose a toolchain based on: (1) *tsfresh* library [34] for generic feature extraction, (2) Naive AutoML [33] for automatically optimizing an ML pipeline that finds both the best model for a dataset and the best preprocessing steps, and (3) adapted forward feature selection to find the most important features. We apply this toolchain to *Hedera helix* electrical differential potentials (recorded using our *PhytoNode*), while the plant is exposed to ozone. We show that our toolchain also works on different plant species and other stimuli using data from *Buss et al.* [22].

In summary, we contribute to implementing low-cost air-pollution monitoring systems based on phytosensing by show-

⁴threshold value for ozone of 60 ppb (parts per billion), e.g. German Federal Environment Agency: <https://www.umweltbundesamt.de/daten/luft/ozon-belastung#zielwerte-und-langfristige-ziele-fur-ozon>

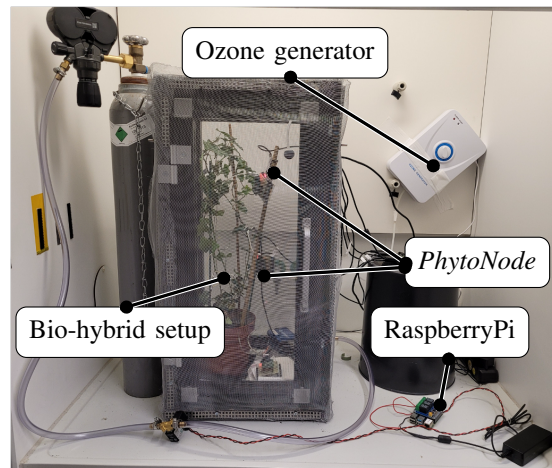


Fig. 1. Experimental setup to expose an ivy plant to ozone. The ivy plant is within a Faraday cage to minimize external disturbances. We use two *PhytoNodes* [7] to measure the plant electric differential potential and a RaspberryPi to store the data. Ozone is generated and induced from the top. The ozone concentration is controlled via two ozone sensors (one at the top and one at the bottom).

ing that

- we can classify ozone exposure in plant physiology in a new plant (*Hedera helix*) with high accuracy;
- developed low-cost hardware (*PhytoNode*) is capable of capturing the relevant signal dynamics necessary for classifying pollutants exposure; and
- our approach can generalize to other plant species and stimuli.

These advances in phytosensing technology, in combination with the present or future urban landscaping, would potentially allow for large-scale outdoor deployment of inexpensive and robust air-quality sensors to effectively monitor air pollution in urban areas. To ensure reproducibility, we have publicly released the code.⁵

II. EXPERIMENTS AND METHODOLOGY

Next, we describe the experimental setup (Sec. II-A), the obtained data, and how we preprocessed it. We describe our toolchain, consisting of deriving plant species and stimulus generic features from the electric differential potential using the *tsfresh* library (Sec. II-B), followed by using these generic features to find and optimize a machine learning model using the Naive AutoML framework (Sec. II-C), and finally employing an adapted forward feature selection to find good working feature subsets (Sec. II-D).

A. Experimental setup

In Fig. 1 we show the experimental setup for the ozone experiments [7]. We use two *PhytoNodes* to simultaneously measure the electric differential potentials close to the leaves and roots with a frequency of approximately 300 Hz. Each *PhytoNode* has a pair of electrodes that are inserted approximately 15 cm apart into the plant's tissue. To reduce

⁵https://github.com/tilly111/watchplant_classification

external disturbances (e.g., electrical noise and static charges), we measure inside a Faraday cage. The ivy plant is exposed to 10 minutes of increased ozone concentration (peak exposure mean $1,447 \text{ ppb} \pm 376 \text{ ppb}$; no exposure mean $-14 \text{ ppb} \pm 52 \text{ ppb}$, negative values due to calibration of the sensors). Then we allow the plant to recover for 2 hours before iterating and exposing it to ozone again. We exposed four different ivy plants to ozone for 17, 19, 18, and 24 repetitions respectively. This yields a total number of 78 *expositions*.

For the class of *no ozone* (i.e., no increased ozone application) we select the 10 minutes right before the ozone exposition. Hence, we have a fully balanced dataset of 156 ten minute slices of electric differential potential of ivy plants, 78 instances with and 78 instances without ozone exposition.

The measurements of the expositions are organized in three datasets. One with the signals received in the plant leaves (*Leaf* dataset), and one with the signals received in the plant stem (*Stem* dataset). We also consider the combined (and time-wise aligned) data (*Combined* dataset).

From these datasets, we remove measurements of those expositions in which the majority of the signal was not recorded. This is the case for 2 expositions (4 samples) in both the leaf and stem measurements of the first plant and 15 expositions (30 samples) of the stem measurements of the second plant. So we have 152 samples of leaf measurements, 122 samples of stem and combined measurements.

We split each of the three datasets (*Leaf*, *Stem*, and *Combined*) randomly into an analysis dataset consisting of 80% of all the data (across plants) and a test dataset consisting of the remaining 20%. For the subsequent processing and analysis, only the analysis datasets are used, if not stated explicitly otherwise.

B. Data preprocessing and feature extraction

First, both leaf and stem measurements are converted from raw sensor readings to millivolt (mV). This transformation allows to eliminate all physically illogical values by removing all electric differential potential measurements that exceed a threshold of $\pm 200 \text{ mV}$. Next, we employ a preprocessing pipeline inspired by *González I. Juclà et al.* [18] that includes a rolling median filter with window size 10, sampling the data down to 2 Hz, and finally cutting the data into 10 minute slices. From each exposition we use the 10 minutes during which the stimulus was applied, the 10 minutes directly before the stimulus application, and 10 to 20 minutes before stimulus application for background subtraction, see Fig. 2. From each 10 minute slice we calculate 787 features using the *tsfresh* library [34]. We chose *tsfresh* because it describes generic time series features, which are applicable for finding a generic and robust solution. Background subtraction is used to mitigate inter-plant variance [22], [24] and is calculated by

$$\text{feature}_{\text{sub}} = \text{feature}_{\text{ozone or no ozone}} - \text{feature}_{\text{background}}.$$

Hence, each sample of the *Leaf* and *Stem* dataset consists of 787 features. The *Combined* dataset consists of 1,502 features

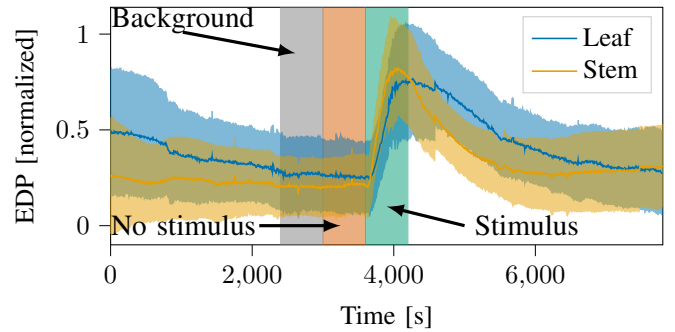


Fig. 2. Example data of the first experiment with 17 expositions. The solid lines show the mean scaled electric differential potential (EDP) over all expositions of the ivy plant (blue at the leaf, orange at the stem). The shaded areas give the standard deviation. The green time interval shows the ten minute slice selected for calculating the stimulus features, the red time interval shows the ten minute slice selected for calculating the no stimulus features, and the gray time interval indicates the ten minute slices used for background subtraction.

as we remove constant features (i.e., same value across all samples).

C. Automated model finding

We use the Naive AutoML library [33] to find the optimal machine learning pipeline for our data in a binary classification task using all features. This library searches in *scikit learn* [35] classifier and preprocessing implementations for the classification pipeline that minimizes or maximizes a given metric. Optimization is greedy in two phases by (1) finding the best algorithm combination of pre-processors and classifiers under default hyperparameters through enumeration and (2) optimizing the hyperparameters of the selected algorithms through random search (e.g., randomly selecting hyperparameters until a valid configuration is found in the default hyperparameter search space of Naive AutoML). Once a pre-defined number of optimization steps has been executed, the best found pipeline is trained on the full dataset and returned. While the greedy decisions could, in principle, lead to sub-optimal pipelines, it was shown empirically that the solutions generally have no or only a very small performance gap to solutions returned by time-intensive methods [33].

This library is easy to configure by allowing to set timeout limits, maximum number of hyperparameter iterations, or evaluation metrics. We do not set a timeout limit but allow only 100 hyperparameter optimization steps (default parameter).

For evaluating our model we run Naive AutoML once with each of two metrics. One run was with the receiver operating characteristics area under the curve (ROC AUC) as we have a binary classification problem, and it is important to incorporate uncertainty of the classifier into the evaluation. ROC AUC captures this uncertainty. In a second run, we optimized for accuracy (ACC), because it will ultimately be the essential measure for our envisioned application. In both cases, Naive AutoML was configured to evaluate pipelines based on 5 independent and stratified 80%/20% training/validation splits.

TABLE I

RESULTS OF THE AUTOMATED MODEL FINDING USING NAIVE AUTOML.
 RFC: RANDOM FOREST CLASSIFIER; KNN: K-NEAREST NEIGHBOR
 CLASSIFIER; HGB: HISTGRADIENTBOOSTING CLASSIFIER; GUS:
 GENERIC UNIVARIATE SELECT; ETC: EXTRA TREES CLASSIFIER.

Dataset	Metric	Score	Best model	Preprocessing
Leaf	Accuracy	0.8880	RFC	Variance Threshold
Stem	Accuracy	0.7800	kNN	Min-max Scalar
Combined	Accuracy	0.9900	HGB	None
Leaf	ROC AUC	0.9654	RFC	None
Stem	ROC AUC	0.8560	ETC	Normalizer
Combined	ROC AUC	0.9333	ETC	None

D. Feature selection

Based on the optimized classification pipeline, we investigate what subset of features performs best. Therefore, we do a semi-greedy approach, where we do 787 feature selection rounds (or 1,502 in the case of the *Combined* dataset). Each round consists of the following steps: (1) we sequentially iterate through all available features (not yet selected features), (2) evaluate the performance for each choice (averaged over 100 independent runs), and (3) add the feature to the set of selected features if it maximizes the performance. To allow for some temporary suboptimality, we keep a number of n best selected feature sets for every feature set size. For each selected feature set, we iterate through all available features in the next round of feature selection. For the first 40 selected features we keep the 10 best feature sets; for selected features 41 to 100 we keep the 5 best feature sets; and after 100 selected features the 3 best feature sets. As performance measure we choose ROC AUC, because it not only considers definite predictions but also scores the certainty of the classifier.

III. RESULTS AND DISCUSSION

Following the experimental protocol described in the previous section, we now describe the relevant intermediate and final results in three steps. First, Sec. III-A details the results of the model selection phase from Naive AutoML. Second, Sec. III-B gives insights into the learning behavior of the selected pipelines in terms of feature and learning curves. Sec. III-C assesses selected models on test data and provides an unbiased estimator for the generalization performance.

A. Model selection

Table I summarizes the best found pipelines (preprocessing plus classifier) depending on the metric used for optimization (either ROC AUC or accuracy). The performance is reported as the average observed in the 5-fold hold-out validation as described in Sec. II-C. We notice that ensemble classifiers (e.g., random forest classifier, extra tree classifier) work well, as they are often selected by Naive AutoML. See our implementation for the hyperparameter sets. However, the performance is generally similar among these models, and due to the small size of the training data, model selection is subject to significant noise and may change if optimization is repeated. For larger datasets, we would expect more consistent model selection because noise and variability are mitigated.

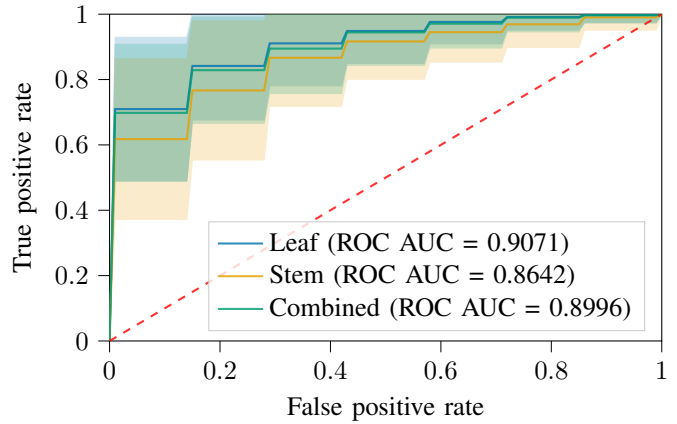


Fig. 3. Each ROC curve is averaged (solid line) over 500 splits using 80%/20% stratified shuffle split and all features of the analysis datasets (blue: leaf, orange: stem, and green: combined). The shaded area corresponds to the standard deviation. The suggested pipeline from Table I is used for each setting.

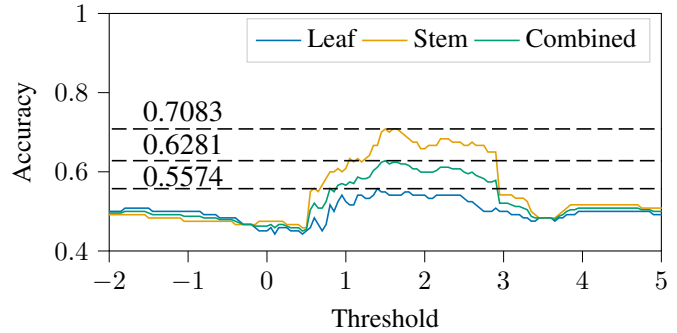


Fig. 4. Accuracy results for a simple threshold model (blue: leaf, orange: stem, and green: combined). The model is evaluated using all experiment data and the result is averaged over 500 independent runs with a random 80%/20% train/validation split. See our implementation for details.

Next, Fig. 3 shows the ROC curves for the pipelines from Table I. To ensure robust interpretation, the curves are obtained from 500 repeated evaluations of the pipeline with independent and stratified 80%/20% splits of the analysis data. One can see that classification is more successful using the leaf data (ROC AUC = 0.9071, ACC = 82.15%) rather than the stem signal (ROC AUC = 0.8642, ACC = 77.51%). Using both signals (e.g., information from the leaf and close to the root) yields a similar separability performance as solely using the leaf signal (ROC AUC = 0.8996, ACC = 83.49%). We observe high variance in the results (shaded areas), which can be attributed to the small training (and validation) set sizes.

For comparison, we show a simple threshold model in Fig. 4. The signal is preprocessed, randomly split into 80% training and 20% validation data and we obtain a maximum accuracy of 70.83% using the stem dataset. Hence, classification is not trivial and the complexity can be explained by varying electric differential potential levels depending on the

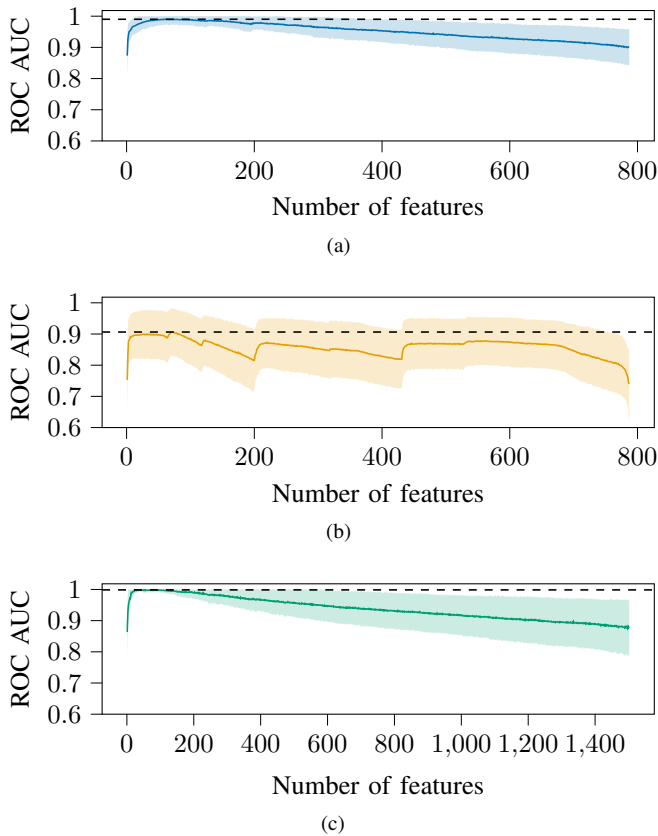


Fig. 5. Mean ROC AUC score (solid line) for the all feature subsets of the (a) leaf, (b) stem, and (c) combined analysis dataset. The best performance is reached using (a) 62 features (AUC ROC score of 0.9901) for the leaf analysis dataset, (b) 69 features (AUC ROC score of 0.9063) for the stem analysis dataset, and (c) 94 features (AUC ROC score of 0.9985) for the combined analysis dataset. Shaded area is the standard deviation.

daytime due to the plant’s system potential [36], [37]. Possibly due to system complexity, plants may respond physiologically individually different to the same external stimulus.

B. Features selection

Based on the pipeline that is best using *all* features, we analyze which feature subsets to choose and if it can further improve the performance of the ML models. This analysis is based on ROC AUC.

In Fig. 5 we show the ROC AUC scores as a function of the feature set size, where feature sets are determined using the selection approach described in Sec. II-D. The best score for the *Leaf* (ROC AUC = 0.9901, ACC = 94.60%), *Stem* (ROC AUC = 0.9063, ACC = 82.64%), and *Combined* analysis dataset (ROC AUC = 0.9985, ACC = 89.34%) is reached using 62, 69, and 94 features, respectively. All results are averaged over 100 independent repetitions (analysis data were randomly split into 80%/20% training and validation data). Generally, good performance is reached with a small subset of features and gradually decreases for larger feature sets. For each dataset, using a smaller subset of features can increase the ROC AUC score compared to using all features (Δ *Leaf*: 0.0894, Δ *Stem*: 0.0421, and Δ *Combined*: 0.0989).

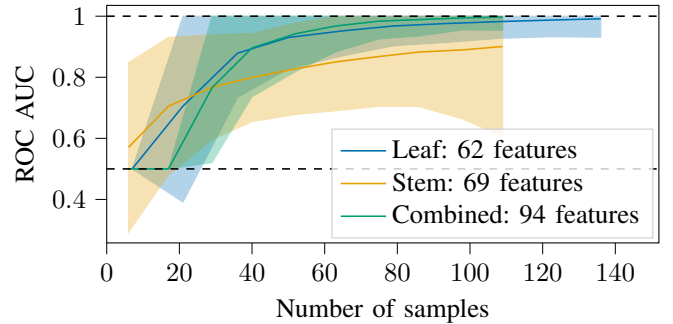


Fig. 6. Learning curves for classifiers trained with (blue) 62 features of the leaf, (orange) 69 features of the stem, and (green) 94 features of the combined analysis dataset. Shaded area is three times the standard deviation. The results are averaged over 500 independent runs (80%/20% random training test split).

This maybe counter-intuitive finding can be explained by the scarcity of training data, which is much smaller than the number of features generated with *tsfresh*, which is also a possible explanation for the noncontinuous behavior of the stem feature subsets (Fig. 5b).

We plot the learning curves for all three datasets while using the best performing feature subset based on the analysis data in Fig. 6. All datasets show a logarithmic behavior, especially the *Leaf* and *Combined* dataset approximate 1.

The high variance (shaded areas are 3 standard deviations) in the *Stem* learning curve can be likely attributed to the fact that the measurements are either generally less informative or more vulnerable to noise than measurements in the leaf. While variance can generally also be attributed to a small dataset, the combined dataset has the same number of samples and does not show such a high variance. Since the combined dataset has access to the leaf measurements, these are preferred over the stem measurements, which explains the more stable behavior of the combined curve.

The relatively high variance in all of the curves suggests that one must be prepared for significant deterioration of performance on the test data (and more generally on new data). Specifically on the *Stem* dataset, one can see that the variance increases towards the full dataset size, and since the final model will be trained on the full analysis data (beyond the curve end in the figure), even higher variance must be expected out of the analysis data. Improvements in test data are theoretically possible but would be unexpected after a massive optimization process, which might have introduced meta overfitting on a small dataset.

C. Generalizability

Finally, we test how the found feature subsets and classifier pipelines perform on the test data. In Fig. 7a, we show the ROC curves for all datasets using all features (similar setting to Fig. 3). While the ROC AUC slightly decreases for the *Leaf* (Δ : 0.0292) and *Combined* (Δ : 0.0089) dataset, it minimally increases for the *Stem* dataset (Δ : -0.0081). The accuracies decrease to 73.26% (*Leaf*), 74.19% (*Stem*), and 70.97% (*Combined*).

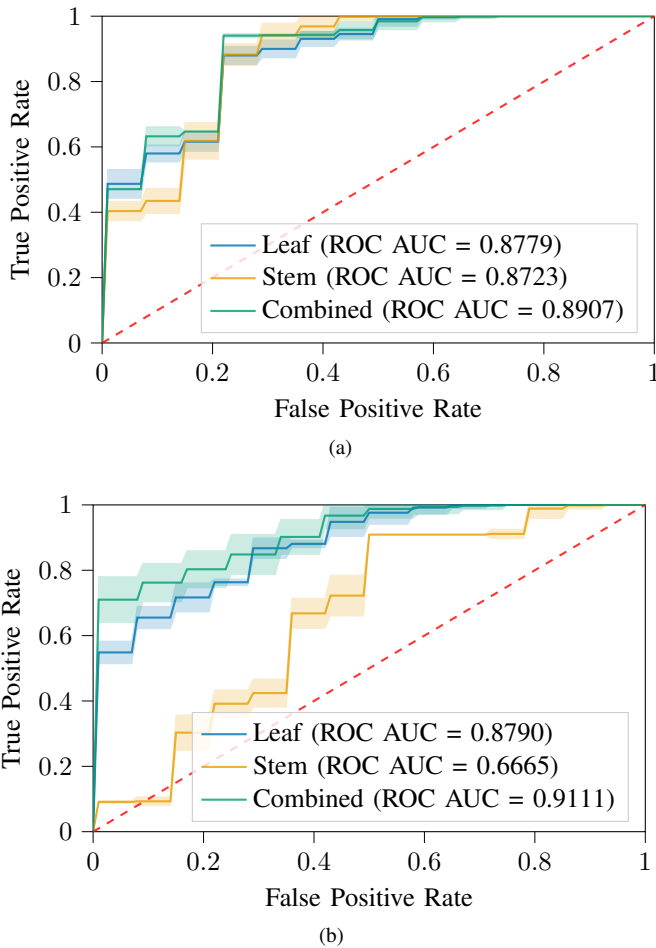


Fig. 7. ROC curves for the test data using (a) all features (same setting as Fig. 3) and (b) the best subset found using the analysis data (62, 69, 94 features respectively, compare Fig. 5). Each curve is averaged over 500 independent runs where all analysis data was used for training and the test data are used for testing.

In Fig. 7b we show the ROC curves for all datasets using the suggested sub feature sets (see Fig. 5). While the average ROC AUC score extremely decreases (Δ : 0.2058) for the *Stem* data, what could be expected due to the presented learning curve in Fig. 6, it slightly increases for the *Leaf* (Δ : 0.011) and *Combined* (Δ : 0.0204) data. The accuracies align and decrease to 57.21% for the *Stem* data, and slightly increase to 76.96%, and 77.30% for the *Leaf* and *Combined* data. The classification results with a high accuracy (up to 83.49% or 94.60% with feature selection on the analysis data) show that our proposed methodology is suitable for classifying ozone stress of ivy plants using their electrophysiology. It also confirms that our developed *PhytoNode* hardware is able to capture the relevant information in said signal. The decline in accuracy on the test data can be explained by meta overfitting, that is, we overfitted the ML pipeline. This also holds for the feature selection as it does not generalize reliable.

The classification results show that measurements close to the leaf are better classifiable, thus exhibiting a clearer response, which aligns well with the intuition that ozone is

absorbed by the leaves (as they ‘breathe’ the ozone), resulting in a clearer and faster reaction in the plant. However, it can be beneficial to measure plant electrophysiological signals at multiple locations.

IV. APPLICATION TO OTHER SPECIES AND STIMULI

Finally and to assess the replicability of the proposed toolchain, we repeated the presented process on separate data of electric differential potential data of ‘ZZ’ plants (*Zamioculcas zamiifolia*, family Araceae) exposed to other stimuli, using different sensing technology (CYBRES phytosensor [38]) [22]. While we spare details of the results for space reasons, we can report classifying accuracy between wind or no wind stimulus of 95.39% using the extra trees classifier and no preprocessing step on unseen test data. This indicates the generalizability of our toolchain.

V. CONCLUSION AND OUTLOOK

We presented an automatic toolchain to classify external stimulus on a plant using the plant’s electric differential potential signal. We propose to calculate generic time series features using the *tsfresh* library to be generic towards plant species and environmental stimuli. For finding a model, we propose to use Naive AutoML a tool that automatically finds and optimizes your machine learning pipeline. The results show that this toolchain can be used to build and train models for different plant species and stimuli to achieve high accuracies. We conclude that, for ozone stress, the best response is measured close to the plant’s leaves and that incorporating additional measurement points can enhance the detection capability.

This generic toolchain allows for easily adjusting your prediction model to new plants as well as stimuli influencing the plant. With this in mind we can use this approach to prototype models which we can later use on the *PhytoNode* to do real-time monitoring of air-pollution in cities using natural plants as sensors.

Next steps include integrating our findings into a real-world application, for example, onboard classification of ozone stress using the *PhytoNode*. To ensure practical applicability, we must confirm that our models also work at lower ozone concentrations commonly encountered in everyday urban environments. We plan to include other relevant pollutant gases and start experimenting also on longer timescales (e.g., hours or days). The proposed automatic toolchain will simplify the integration of all these factors. We will consider also deep learning approaches; however, non-deep learning approaches seem more efficient and feasible in terms of space or computing complexity, considering a light-weight device, such as the *PhytoNode*. We hope our toolchain will enable inexpensive scalable, real-time air-quality sensors and contribute to more effective and sustainable urban environmental monitoring.

ACKNOWLEDGMENT

This work is supported by EU H2020 FET project Watch-Plant, grant agreement No. 101017899 and the project ING-312-2023 at Universidad de La Sabana.

REFERENCES

- [1] S. L. Ullo and G. R. Sinha, "Advances in smart environment monitoring systems using iot and sensors," *Sensors*, vol. 20, no. 11, p. 3113, 2020.
- [2] X. Xie, I. Semanjski, S. Gautama, E. Tsiligianni, N. Deligiannis, R. Rajan, F. Pasveer, and W. Philips, "A review of urban air pollution monitoring and exposure assessment methods," *ISPRS International Journal of Geo-Information*, vol. 6, no. 12, p. 389, 2017.
- [3] E. G. Snyder, T. H. Watkins, P. A. Solomon, E. D. Thoma, R. W. Williams, G. S. Hagler, D. Shelow, D. A. Hindin, V. J. Kilaru, and P. W. Preuss, "The changing paradigm of air pollution monitoring," *Environmental Science & Technology*, vol. 47, no. 20, pp. 11 369–11 377, 2013.
- [4] L. García-Carmona, S. Bogdan, A. Diaz-Espejo, M. Dobielewski, H. Hamann, V. Hernandez-Santana, A. Kernbach, S. Kernbach, A. Quijano-López, N. Roxhed, B. Salamat, and M. Wahby, "Biohybrid systems for environmental intelligence on living plants: WatchPlant project," in *Proceedings of the Conference on Information Technology for Social Good*, ser. GoodIT'21, 2021, pp. 210–215.
- [5] H. Hamann, S. Bogdan, A. Diaz-Espejo, L. García-Carmona, V. Hernandez-Santana, S. Kernbach, A. Kernbach, A. Quijano-López, B. Salamat, and M. Wahby, "WatchPlant: Networked bio-hybrid systems for pollution monitoring of urban areas," in *ALIFE 2022: The 2022 Conference on Artificial Life*, vol. ALIFE 2021: The 2021 Conference on Artificial Life, 2021, pp. 37–45.
- [6] E. Buss, T.-L. Rabbel, V. Horvat, M. Križmančić, S. Bogdan, M. Wahby, and H. Hamann, "Phytonodes for environmental monitoring: Stimulus classification based on natural plant signals in an interactive energy-efficient bio-hybrid system," in *Proceedings of the 2022 ACM Conference on Information Technology for Social Good*. ACM, 2022, pp. 258–264.
- [7] E. Buss, T. Aust, O. Hamburger, C. K. Heck, and H. Hamann, "Phytonode upgraded: Energy-efficient long-term environmental monitoring using phytosensing," in *Advances in Information and Communication. FICC 2025. Lecture Notes in Networks and Systems*. Springer Nature Switzerland, 2025, (in press).
- [8] A. C. Pfothenauer and S. C. Lenaghan, "Phytosensors: Harnessing plants to understand the world around us," *Current Opinion in Biotechnology*, vol. 87, p. 103134, 2024.
- [9] E. Sukhova, E. Akinchits, and V. Sukhov, "Mathematical models of electrical activity in plants," *The Journal of Membrane Biology*, vol. 250, no. 5, pp. 407–423, 2017.
- [10] M. I. Jordan and T. M. Mitchell, "Machine learning: Trends, perspectives, and prospects," *Science*, vol. 349, no. 6245, pp. 255–260, 2015.
- [11] Y. LeCun, Y. Bengio, and G. Hinton, "Deep learning," *nature*, vol. 521, no. 7553, pp. 436–444, 2015.
- [12] L. Tian, C. Shang, M. Li, and Y. Wang, "Research on classification of water stress state of plant electrical signals based on pso-svm," *IEEE Access*, vol. 11, pp. 125 021–125 032, 2023.
- [13] K. Sai, N. Sood, and I. Saini, "Time series data modelling for classification of drought in tomato plants," *Theoretical and Experimental Plant Physiology*, vol. 35, pp. 379–394, 2023.
- [14] E. Najdenovska, F. Dutoit, D. Tran, C. Plummer, N. Wallbridge, C. Camps, and L. E. Raileanu, "Classification of plant electrophysiology signals for detection of spider mites infestation in tomatoes," *Applied Sciences*, vol. 11, no. 4, 2021.
- [15] D. Tran, F. Dutoit, E. Najdenovska, N. Wallbridge, C. Plummer, M. Mazza, L. E. Raileanu, and C. Camps, "Electrophysiological assessment of plant status outside a Faraday cage using supervised machine learning," *Scientific Reports*, vol. 9, no. 1, p. 17073, 2019.
- [16] X.-H. Qin, Z.-Y. Wang, J.-P. Yao, Q. Zhou, P.-F. Zhao, Z.-Y. Wang, and L. Huang, "Using a one-dimensional convolutional neural network with a conditional generative adversarial network to classify plant electrical signals," *Computers and Electronics in Agriculture*, vol. 174, p. 105464, 2020.
- [17] J.-P. Yao, Z.-Y. Wang, R. F. de Oliveira, Z.-Y. Wang, and L. Huang, "A deep learning method for the long-term prediction of plant electrical signals under salt stress to identify salt tolerance," *Computers and Electronics in Agriculture*, vol. 190, p. 106435, 2021.
- [18] D. González I Juclá, E. Najdenovska, F. Dutoit, and L. E. Raileanu, "Detecting stress caused by nitrogen deficit using deep learning techniques applied on plant electrophysiological data," *Scientific Reports*, vol. 13, p. 9633, 2023.
- [19] J. Qi, C. Liu, Q. Wang, Y. Shi, X. Xia, H. Wang, L. Sun, and H. Men, "Clivia biosensor: Soil moisture identification based on electrophysiology signals with deep learning," *Biosensors and Bioelectronics*, vol. 262, p. 116525, 2024.
- [20] D. R. Pereira, J. P. Papa, G. F. R. Saraiva, and G. M. Souza, "Automatic classification of plant electrophysiological responses to environmental stimuli using machine learning and interval arithmetic," *Computers and Electronics in Agriculture*, vol. 145, pp. 35–42, 2018.
- [21] K. Sai, N. Sood, and I. Saini, "Abiotic stress classification through spectral analysis of enhanced electrophysiological signals of plants," *Biosystems Engineering*, vol. 219, pp. 189–204, 2022.
- [22] E. Buss, T. Aust, M. Wahby, T.-L. Rabbel, S. Kernbach, and H. Hamann, "Stimulus classification with electrical potential and impedance of living plants: Comparing discriminant analysis and deep-learning methods," *Bioinspiration & Biomimetics*, vol. 18, no. 2, p. 025003, 2023.
- [23] S. L. Chaparro-Cárdenas, J. A. Ramirez-Bautista, W. Gamboa-Contreras, A. L. Moreno-Chacón, and F. C. Vargas-Tangua, "Plant electrophysiology: Bibliometric analysis, methods and applications in the monitoring of plant-environment interactions," *Dyna*, vol. 88, no. 218, pp. 212–223, 2021.
- [24] S. K. Chatterjee, S. Das, K. Maharatna, E. Masi, L. Santopolo, S. Mancuso, and A. Vitaletti, "Exploring strategies for classification of external stimuli using statistical features of the plant electrical response," *Journal of the Royal Society Interface*, vol. 12, no. 104, p. 20141225, 2015.
- [25] S. K. Chatterjee, S. Das, K. Maharatna, E. Masi, L. Santopolo, I. Colzi, S. Mancuso, and A. Vitaletti, "Comparison of decision tree based classification strategies to detect external chemical stimuli from raw and filtered plant electrical response," *Sensors and Actuators B: Chemical*, vol. 249, pp. 278–295, 2017.
- [26] S. K. Chatterjee, O. Malik, and S. Gupta, "Chemical sensing employing plant electrical signal response-classification of stimuli using curve fitting coefficients as features," *Biosensors*, vol. 8, no. 3, 2018.
- [27] N. Bhadra, S. K. Chatterjee, and S. Das, "Multiclass classification of environmental chemical stimuli from unbalanced plant electrophysiological data," *PLOS ONE*, vol. 18, no. 5, pp. 1–31, 2023.
- [28] M. Dolfi, I. Colzi, S. Morosi, E. Masi, S. Mancuso, E. Del Re, F. Francini, and R. Magliacani, "Plant electrical activity analysis for ozone pollution critical level detection," in *2015 23rd European Signal Processing Conference (EUSIPCO)*. IEEE, 2015, pp. 2431–2435.
- [29] Q. Yao, M. Wang, Y. Chen, W. Dai, Y.-F. Li, W.-W. Tu, Q. Yang, and Y. Yu, "Taking human out of learning applications: A survey on automated machine learning," *arXiv preprint arXiv:1810.13306*, vol. 31, 2018.
- [30] M. Feurer, A. Klein, K. Eggenberger, J. Springenberg, M. Blum, and F. Hutter, "Efficient and robust automated machine learning," in *Advances in Neural Information Processing Systems 28*, 2015, pp. 2962–2970.
- [31] M. Feurer, K. Eggenberger, S. Falkner, M. Lindauer, and F. Hutter, "Auto-sklearn 2.0: Hands-free automl via meta-learning," *Journal of Machine Learning Research*, vol. 23, no. 261, pp. 1–61, 2022.
- [32] P. Gijsbers and J. Vanschoren, "GAMA: Genetic automated machine learning assistant," *Journal of Open Source Software*, vol. 4, no. 33, 2019.
- [33] F. Mohr and M. Wever, "Naive automated machine learning," *Machine Learning*, vol. 112, pp. 1131–1170, 2022.
- [34] M. Christ, N. Braun, J. Neuffer, and A. W. Kempa-Liehr, "Time series feature extraction on basis of scalable hypothesis tests (tsfresh – a python package)," *Neurocomputing*, vol. 307, pp. 72–77, 2018.
- [35] F. Pedregosa, G. Varoquaux, A. Gramfort, V. Michel, B. Thirion, O. Grisel, M. Blondel, P. Prettenhofer, R. Weiss, V. Dubourg, J. Vanderplas, A. Passos, D. Cournapeau, M. Brucher, M. Perrot, and E. Duchesnay, "Scikit-learn: Machine learning in Python," *Journal of Machine Learning Research*, vol. 12, pp. 2825–2830, 2011.
- [36] J.-H. Li, L.-F. Fan, D.-J. Zhao, Q. Zhou, J.-P. Yao, Z.-Y. Wang, and L. Huang, "Plant electrical signals: A multidisciplinary challenge," *Journal of Plant Physiology*, vol. 261, p. 153418, 2021.
- [37] M. R. Zimmermann, H. Maischak, A. Mithöfer, W. Boland, and H. H. Felle, "System Potentials, a Novel Electrical Long-Distance Apoplastic Signal in Plants, Induced by Wounding," *Plant Physiology*, vol. 149, no. 3, pp. 1593–1600, 2009.
- [38] S. Kernbach, *Differential Impedance Spectrometer for electrochemical and electrophysiological analysis of fluids and organic tissues. Handbook and User Manual*. CYBRES GmbH, Stuttgart, 2022.